Device for Measurement of Human Tissue Properties In Vivo

Robert L. Williams II[1]
e-mail: williar4@ohio.edu

Wei Ji

John N. Howell

Robert R. Conatser, Jr.

Interdisciplinary Institute for
Neuromusculoskeletal Research,
Ohio University,
Athens, Ohio 45701-2979

We present a method for measurement of human tissue compliance in vivo using a commercial haptic interface to apply known step changes in force while recording the resulting displacements. We introduce our system, the soft-tissue compliance meter. Our motivation was to improve the compliance realism of our virtual haptic back model, but there are many potential applications for this method. We present calibration of the haptic interface, pseudostatic compliance measurement techniques, measurement of contracted muscle compliances, and several important issues affecting our results.
[DOI: 10.1115/1.2778703]

Keywords: Virtual Haptic Back, in vivo human body compliance measurement, human tissue properties, palpatory diagnosis, haptics, biomechanics

1 Introduction

The NIH-sponsored Visible Human project is useful to teach anatomy.[2] We are interested in generating the virtual palpable human, i.e., a virtual reality model of the live human body with high-fidelity graphics such as the visible human, combined with high-fidelity haptic (force and touch) feedback to the user.

In the Virtual Haptic Back project at Ohio University (Williams et al. [1]), we have a need to measure real, living human tissue compliance properties to ensure maximum realism in our haptic models for manual medicine training. Related fields also require this information: automotive industry, the consumer product industry, physical therapy, and digital human modeling in general. Many biomedical engineering research groups are creating finite-element-based models of live human body components, but are lacking realistic material properties to use in these models.

The problem we are addressing is how to measure real human body tissue properties accurately and quickly in vivo. The methods should allow for a range of different parts of the body and a range of humans, including adults, seniors, children, females, and males, plus different body types.

In the past, the most common form of human tissue property measurement has been with cadaver-based measurements. Whether the deceased subject was embalmed or not, this method is inadequate for realistically simulating the behavior of live human tissue.

An exception has been in the dental field where a probe may measure tissue compliance in vivo. Noyes and Solt [2] presented Bode plots of mobility (peak force/peak velocity) versus frequency for dental tissue with small forces.

The Center for Integration of Medicine and Innovative Technology (CIMIT) has been measuring the properties of organs for virtual physics-based surgery simulation by removing subject organs and exposing them to mechanical displacements and observing the responding forces.[3] For in vivo measurements, there are currently two options: a noninvasive, image-based method examining the strain fields within living tissues subject to force fields and invasive methods based on measuring the force-displacement responses of tissues (Ottensmeyer [3]). For invasive methods, laparoscopic methods are common, generally using pigs due to their similarity to human organs. Wang et al. [4] have developed a sensor for in vivo analysis of multiple-layer buttock soft tissue to help identify persons subject to pressure ulcers. Edsberg et al. [5] experimented with human skin in vitro via uniaxial tensile testing, reporting the first compressive-preload-induced strain softening of a biological material. EnduraTEC[4] is involved with all kinds of biological and bioengineering materials studies: teeth, vocal cords, cartilage, artificial heart valves and stents, liver, orthotic heel model, and spinal disk implants. However, most of their materials are engineered; of the biological tissue studies, all are in vitro or in animal subjects (pigs and cows).

Bruyns and Ottensmeyer [6] use the TeMPeST 1D, a voice-coil-motor-actuated machine to measure force/displacement curves in vitro, to determine the mechanical properties of rat organs to support their Virtual Rat Project. Carter et al. [7] report ex vivo measurements of pig and sheep liver compliance using a static compliance probe and in vivo measurement of human liver compliance using a handheld compliance probe during surgery. Djerad et al. [8] study stress-induced fluid flow in dissected porcine cardiac tissue using poroelasticity theory.

Our patent search yielded three related concepts. Randolph [9] designed a durometer to determine the surface hardness of human tissue for dental and medical use in identifying edema, swelling, puffiness, and distension. Kovacevic [10] invented a handheld device for skin compliance measurements in medical and dental cases where tissues must bear loads or swell after treatment. Neurogenic Technologies, Inc. [11] has developed the Myotonometer®,[5] a handheld measurement system, to determine relative muscle tone, compliance, strength, and spasm.

This article presents experiments to demonstrate our in vivo technique for measuring the compliance of human tissue. Data from this technique can be used (1) to provide realistic haptic properties for the Virtual Haptic Back project at Ohio University, (2) to measure the compliance of patients at various points to support clinical diagnosis and treatment, and (3) to measure human body properties for a range of subjects (varying age, gender, and body type) to support industrial and consumer product design. First, we present haptic interface details, followed by our pseudostatic compliance measurement techniques and results (including compliance measurement of contracted muscles), and then we discuss and present experiments for several important factors in the effectiveness of our measurements.

[1]Corresponding author.
[2]www.nlm.nih.gov/research/visible/visible_human.html
[3]www.medicalsim.org
[4]www.enduratec.com
[5]www.neurogenic.com

Submitted to ASME for publication in the JOURNAL OF MEDICAL DEVICES. Manuscript received November 21, 2006; final manuscript received August 6, 2007. Review conducted by Gerald E. Miller.

Table 1 PHANTOM® 3.0 specifications

Translational workspace	838×584×406
Displacement resolution	0.02 mm
Maximum force	22 N
Continuous force (24 h)	3 N
Compliance	1 mm/N
Backdrive friction	0.2 N
Apparent tip inertia	<159 g
Footprint	203×203 mm^2

2 Commercial Haptic Interface

We have developed a solution for in vivo measurement of the mechanical properties of human tissue compliance in the Virtual Haptic Back Laboratory at Ohio University. The tissue properties required for virtual human models are generally 3D compliance, as defined in Eq. (1). Stiffness is the inverse of compliance; we will generally refer only to compliance in this article. The definitions below are general; they may be adapted for specific X, Y, Z Cartesian directions, one by one, to obtain the general 3D compliance properties. Units are millimeters for displacement and newtons for force so compliance units are mm/N. Human tissue is generally nonlinear, nonhomogeneous, and nonisotropic, greatly complicating the property measurement compared to common engineering materials [12].

AQ: #2

$$\text{compliance} = \frac{\text{displacement}}{\text{force}} \left(\frac{\text{mm}}{\text{N}} \right) \quad (1)$$

Our method uses two commercial haptic interfaces, both PHANTOM® 3.0s (SensAble Technologies, Inc.[6]), to apply forces and measure displacements in our human subjects at desired compliance measurement points. We can measure the compliance of two points simultaneously with both haptic interfaces and we can also do single point measurement with one haptic interface. We refer to our two haptic interfaces as the "left" and "right" PHANTOM 3.0s. This section presents the specifications and calibration of our PHANTOM® 3.0 haptic interfaces.

2.1 PHANTOM® 3.0 Haptic Interface Specifications. From the manufacturer's information, the PHANTOM® 3.0 specifications are reported below. This device is capable of exerting forces in X, Y, Z and measuring displacements in X, Y, Z. It is capable of covering the points of interest on the subject's back without moving the subject, and it is capable of the forces and displacement resolution we need.

2.2 PHANTOM® 3.0 Haptic Interface Calibration. We need reliable X, Y, Z displacement measurements from the PHANTOM® 3.0 with sufficient resolution. Since our displacement measurements are taken relative to the initial tip placement on the human body surface, we do not need absolute accuracy in position measurements. The manufacturer reports a 0.02 mm displacement resolution for the PHANTOM® 3.0 (Table 1), which is adequate for our purposes.

Our in vivo compliance measurement methods include exerting force step inputs via the PHANTOM® 3.0 in steps of 0.5 N, 1 N, 2 N, 3 N, 4 N, 5 N, and 6 N. Our force calibration technique prior to each experiment is to command the PHANTOM® 3.0 to exert these levels of force on an external force transducer and ensure that the desired force levels are achieved. This force transducer is the ultra precision miniload cell MDB-2.5 from Transducer Techniques, Temecula, CA. The resolution of the force transducer is 0.006 N. All data reported in this article passed this force calibration test within 0.05 N of the desired absolute force, at all force levels directly prior to data collection in each case.

[6]www.sensable.com

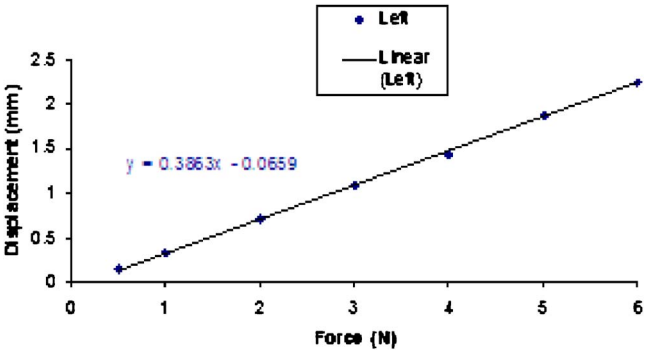

Fig. 1 Left PHANTOM experimental compliance

We also need to calibrate the compliance of the PHANTOM® 3.0 itself because it is not rigid. Since we are measuring the compliance of the human body, we need to know the compliance of the measuring device since it could affect our results. The less compliant the measuring device relative to the human body compliance, the better. Figure 1 shows the results of a calibration experiment wherein the left PHANTOM® 3.0 was commanded to exert the step inputs of force (0.5 N, 1 N, 2 N, 3 N, 4 N, 5 N, and 6 N), increasing the force level every 1.5 s while pushing on a rigid surface. We expect zero displacement since the surface is rigid; the displacements evident in Fig. 1 are due to the compliance of our left PHANTOM® 3.0. A linear fit is made to these data resulting in a compliance of 0.39 mm/N (the slope) with a small y intercept. Averaging four such calibration experiments for the left and also right PHANTOM® 3.0s yield average compliance values of 0.37 mm/N for our left and 0.44 mm/N for our right PHANTOM® 3.0s. From Table 1, the manufacturer states that the compliance is 1 mm/N. The manufacturer must be quoting worst-case compliance results since our measurements, taken near the middle of the workspace, indicate that the PHANTOM® 3.0s are significantly less compliant, which benefits our measurements.

If the PHANTOM® 3.0 is significantly less compliant than the human tissue measured, there will be little error due to this internal measuring device compliance. Assuming a simple series spring model with the applied force acting through the PHANTOM® 3.0 in series with the human tissue, the overall equivalent compliance is

$$C_{\text{eq}} = C_P + C_H \quad (2)$$

We can find the human tissue compliance C_H from $C_H = C_{\text{eq}} - C_P$, where the equivalent compliance C_{eq} is measured (see methods below) and the PHANTOM® 3.0 compliances C_P were stated above for our left and right PHANTOM® 3.0s. Note that Eq. (2) applies to elastic systems but not necessarily viscoelastic systems such as human tissue. Therefore, Eq. (2) may oversimplify and should be improved in the future.

3 Compliance Measurement Methods

To date, we have used this in vivo human tissue compliance measurement technique for the back, the abdomen, and various points measured for clinical muscle tension studies. In this article, we will focus on back compliance measurements.

3.1 Static Back Compliance Measurement Methods. For our method, the first step is to mark the landmarks at which we wish to measure tissue properties of the subject. The tissue property measurement method is shown in Fig. 2. The subject is prone in this case and we are measuring surface properties of the back at vertebra T7 (this article uses the standard notation of Tn for the nth thoracic vertebra, plus C for cervical and L for lumbar vertebrae). The seated operator has placed the tip of the PHANTOM® 3.0, fitted with a rounded probe the size of a finger pad (partial sphere,

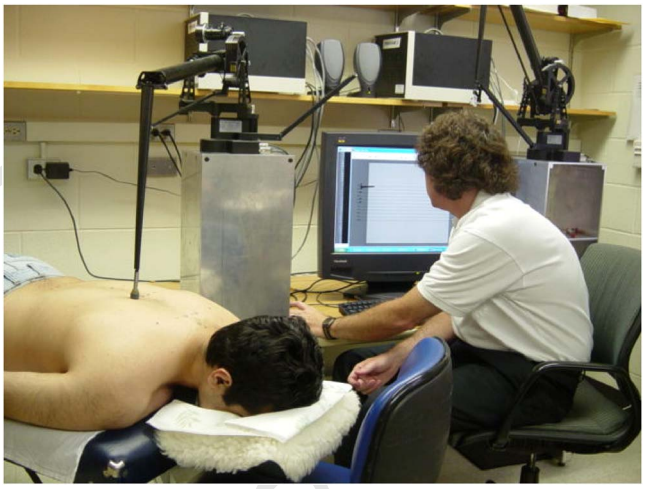

Fig. 2 Back compliance measurement method

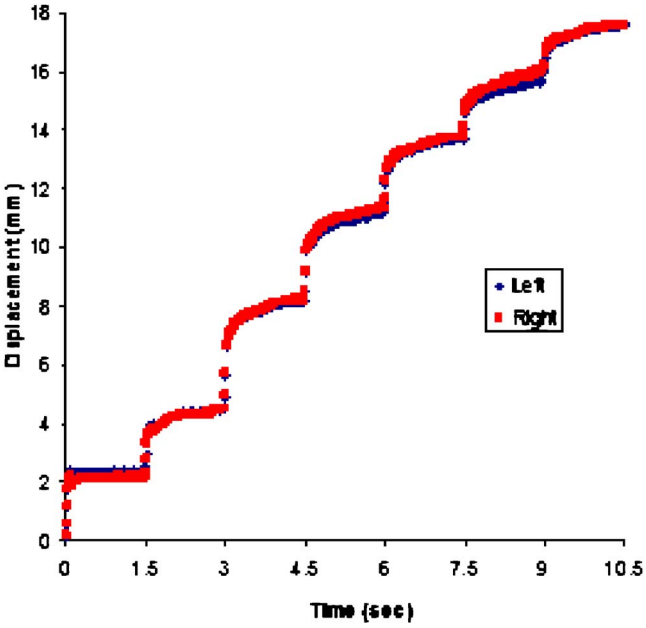

Fig. 3 Data for cervical-region compliance measurement

10 mm diameter), at the desired location. The haptic interface is commanded to exert seven increasing step levels of force (0.5 N, 1 N, 2 N, 3 N, 4 N, 5 N, and 6 N exerted every 1.5 s). For each force, the displacement into the back is measured by the haptic interface encoders and forward displacement kinematics and recorded by the system automatically. For static compliance measurements, we take a single displacement value near the end of each 1.5 s application time, prior to increasing the input force to another step and repeating the process, while the subject holds her breath. The resulting displacement data are plotted on the vertical axis versus the force on the horizontal axis. If the result is linear, the slope of this line is the compliance of the back at this point on the subject. If the result is nonlinear, the compliance changes, defined by the slope of the curve at each point. The compliances at this point in the remaining Cartesian directions (in the plane of the back, normal to the direction being measured in Fig. 2) are measured in a similar manner.

We call this system the soft-tissue compliance meter (softcometer). The measurement tool (PHANTOM® 3.0) is calibrated in millimeters and newtons. Breathing can interfere with the compliance measurements. Therefore, the subject is asked to take three deep breaths in succession, then take half a breath and hold it in, closing the glottis and relaxing all muscles. Then, the force is applied and the corresponding displacement recorded. We command the haptic interface to exert the seven force levels every 1.5 s, and the data are recorded automatically during one breath cycle. Each of these specifications is considered in more detail later in this article.

Figure 3 shows a representative in vivo data collection result for a single test on one subject in the cervical vertebra region of the back. Measured displacement is the dependent variable, plotted versus the independent variable time. The effect of the changing force steps every 1.5 s is evident in Fig. 3. At each change in force input, a dynamic displacement change is evident. To date, we only try to capture the pseudostatic behavior of human tissue in vivo. Viscoelastic dynamic models will be considered in future work. To generate compliance curves, we record the displacement near the end of each 1.5 s period, just prior to increasing the force for the next step.

Since backs are 3D surfaces and not flat planes, we have developed a method to command the PHANTOM® to exert force in the normal direction to the back at each measurement point rather than only along a global vertical direction that is not necessarily perpendicular to the back. At each measurement point of interest, we use an angle measuring device to ascertain the angles (in two orthogonal directions) of the surface relative to absolute vertical. Then, these numbers are entered into the program and the forces are exerted in the desired direction, normal to the back.

Now, we present sample data from experiments with the in vivo measurement of back compliance properties using the commercial haptic interfaces. Figure 4 shows the compliance curves (dependent measurement displacement versus independent applied force) for vertebra L3, including the center (S, for spinous process), 4 cm left of center, and 4 cm right of center. Figure 5 shows the compliance curves for vertebra T10, including the center (S), 2 cm left, and 2 cm right.

Both graphs are for compliance normal to the subject's back and include best-fit lines for the data. The compliance with linear fit is the slope of each line. We see in all cases that compliance over the spinous process (S) is fairly linear, while the compliance over the sides is less linear. The L3 compliance (Fig. 4) is approximately 1.21 mm/N over the spinous process and is 2.22 mm/N 4 cm to the left and right. The T10 compliance (Fig. 5) is approximately 1.27 mm/N over the spinous process and is 1.51 mm/N 2 cm to the left and right. The compliance lines left and right of the spine in Fig. 5 are not identical to each other, due to natural asymmetries in the subject's back, but the slopes (i.e.,

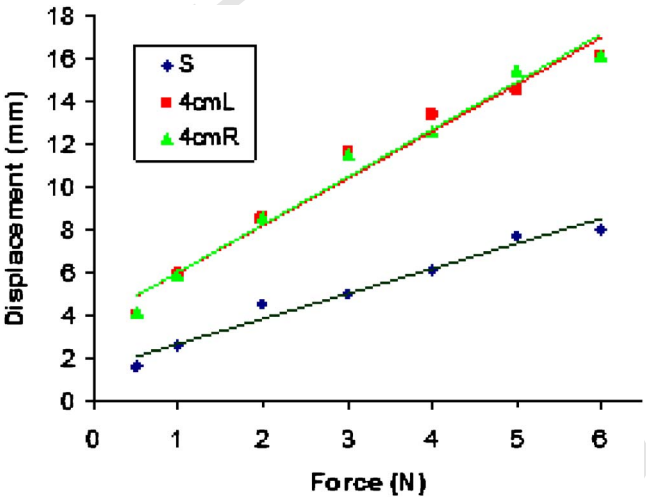

Fig. 4 L3 compliance results

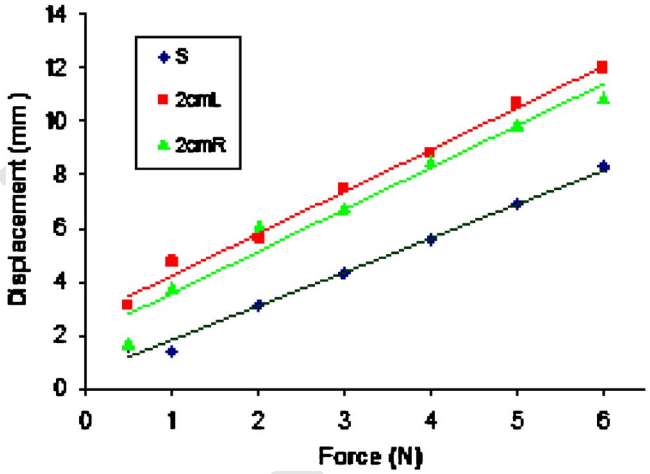

Fig. 5 T10 compliance results

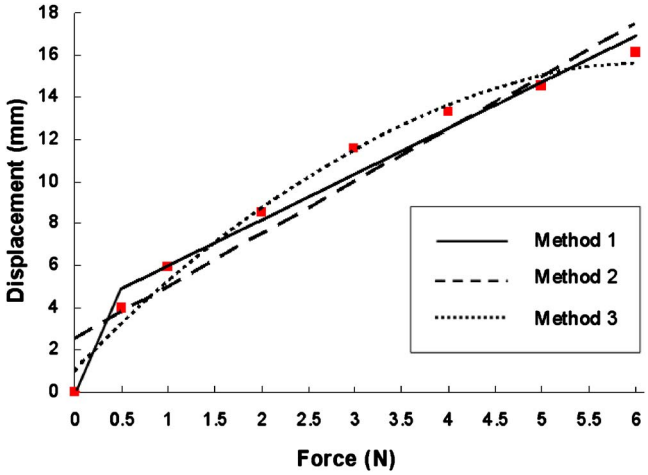

Fig. 6 Improved compliance curves, L3 4 cm L

the compliances) are very similar. From Figs. 4 and 5, we see that regions to the left and right of L3 are more compliant than left and right of T10, but the spinous process compliances of L3 and T10 are roughly the same, which is expected from anatomy. Also, the boney spinous processes in each case are less compliant than the left and right regions, which are muscular.

The spinous process compliances reported above are in the region of 1.2 mm/N; the compliances of the PHANTOM® 3.0 measuring devices are in the region of 0.4 mm/N. The measurements will be less reliable the closer the human body compliances become to the measuring device compliance.

Tables 2 and 3 show the linear regression equations and R^2 values for Figs. 4 and 5, respectively.

In general, the depths of soft tissue above the bony landmarks vary from person to person and amongst the various measuring points on one person. We measured some of these depths using ultrasound on thin to normal-sized subjects. Surface to spinous processes ranged from 5 to 15 mm, depending on the vertebral level. T10 and L3 have depths around 15 mm. T1 and T6–T8 have skin to spinous process depths closer to 5 mm. For 2 cm left and right of the spinous process, depths from skin to bone are between 25 cm and 40 mm. For T10 and L3, these left and right depths are around 35 mm. The cervical-region depths are generally greater, at least 15 mm at the spinous process and at least 35 mm to the left and right.

In Figs. 4 and 5, we see that each of the best-fit straight lines is only for seven data points, one for each force step, i.e., we did not include the implied data point of (0,0). Since the data are nonlinear, this means that the best-fit line does not pass near the origin, which is a valid implied data point. We have three methods to deal with this problem, demonstrated in Fig. 6 for the L3, 4 cm L case of Fig. 4 only, for clarity. (1) We may simply keep the result of Fig. 4 but artificially draw a second line from (0,0) to the left end of the best-fit line, to handle displacements at low force values (less than 0.5 N) with a steeper slope (higher compliance). (2) We may include the data point (0,0) and rederive a new best-fit straight line. (3) We may fit a nonlinear curve to the data, including (0,0)—here we demonstrate a quadratic curve fit. Figure 7 shows the compliances associated with Fig. 6, for the three methods discussed above.

Table 4 summarizes the results from the improved compliance curves shown in Fig. 6. For our virtual haptic back purposes, Method 1 is the best because the best-fit line that does not pass through the origin captures the main compliance behavior in a linear manner, in the force range we need most. This is the method

Table 2 L3 linear regression results for Fig. 4

	Linear regression equation	R^2
S	$y=1.16x+1.50$	0.970
4 cm *L*	$y=2.18x+3.85$	0.970
4 cm *R*	$y=2.20x+3.86$	0.976

Table 3 T10 linear regression results for Fig. 5

	Linear regression equation	R^2
S	$y=1.27x+0.55$	0.991
2 cm *L*	$y=1.57x+2.70$	0.991
2 cm *R*	$y=1.57x+2.00$	0.963

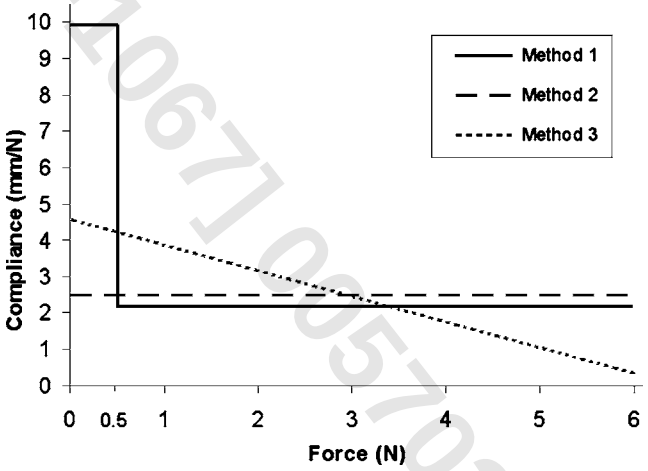

Fig. 7 Compliances from Fig. 6

Table 4 Improved compliance results

Method	Displacement function d	Compliance	r^2
1	$d=990f$ $0\leq f<0.5$	990	NA
	$d=2.18f+3.86$ $f\leq 0.5$	2.18	0.97
2	$d=2.49f+2.54$	2.49	0.94
3	$d=-0.35f^2+4.55f+1.02$	$-0.70f+4.55$	0.99

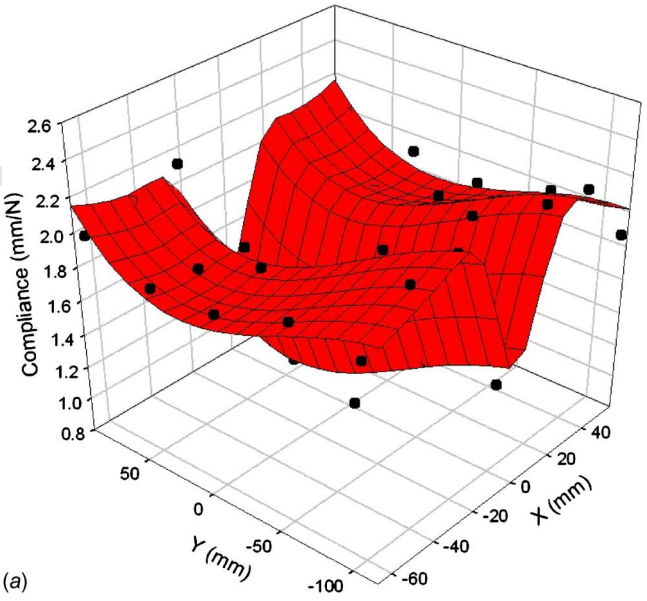

Fig. 8 In vivo back compliance results: (*a*) best-fit surface and (*b*) associated compliance color map

selected in the results presented in this article. However, clearly from Fig. 6, the nonlinear fit to the data is best for nonlinear tissue. The application should dictate the best-curve fitting method.

Clearly, with Method 1, there is a potential problem where the two compliance values change by a step, i.e., we should include a function to smoothly change the compliance in the neighborhood of $f=0.5$ N.

Figure 8 shows a sample result for experimental in vivo back compliance measurements over the entire back of one subject. The same data are shown in two manners, a 3D surface plot (Fig. 8(*a*)) and a color map (Fig. 8(*b*)). In Fig. 8(*a*), X and Y are the independent back coordinates, while the Z data present the dependent compliance measurements. The dots represent actual data points while the surface is a best-fit surface to these points. As expected, the compliance is lowest along the spinal column and then it varies symmetrically as shown for this particular subject. As shown in Fig. 8(*b*), the next lowest compliance regions are along the ribcage. The highest compliances are at the shoulder muscles and in the lower back to the left and right of the spine.

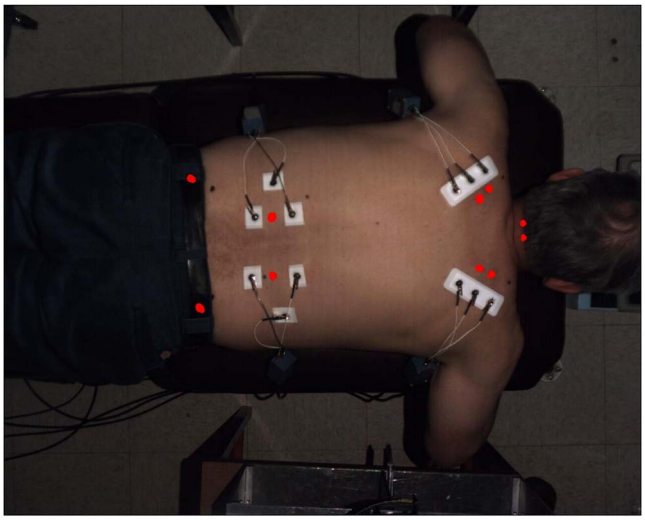

Fig. 9 Measurement points plus EMG leads

3.2 Contracted Muscle Compliance Measurement. In order to demonstrate that our in vivo tissue compliance measurement is effective for determining reduced compliance of muscles in various clinical applications, we conducted the following experiment. Using the same basic methods outlined above, we included EMG leads for voluntary contraction feedback to the subject. We asked our expert subject (Howell) to perform various levels of voluntary contraction of muscles (in the lumbar, cervical, and trapezius regions separately). The subject used the EMG display to hold various levels of voluntary contraction while the haptic interface performed the compliance measurements (all while the subject held his breath). This process is pictured in Fig. 9 (the oscilloscope for EMG readings is not clearly visible under the subject's head).

Figure 10 shows the left and right compliance plots for the lumbar measurement region, for a voluntary contraction equivalent to 100 mV. We see that the data are nonlinear but may be represented by a best-fit line in the force range of 0.5–6 N. Though the displacements allowed in the subject's lumbar region were significantly different (note the y intercepts of Fig. 10), the compliances, i.e., the slopes of the lines in Fig. 10, are similar: 1.35 mm/N for the right and 1.27 mm/N for the left.

From the calibration section, we found experimentally that the compliances of the measuring devices (PHANTOM® 3.0 haptic interfaces) were 0.44 mm/N for our right and 0.37 mm/N for our left PHANTOMS®, a significant fraction of the overall compliance

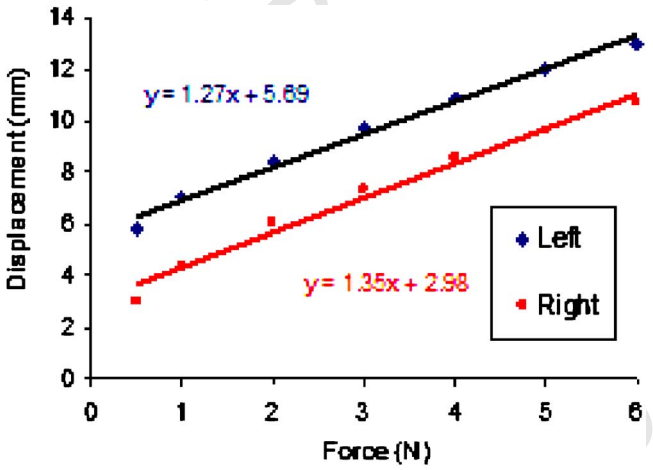

Fig. 10 Lumbar compliance plots, 100 mV contraction

PROOF COPY [MED-06-1067] 005703MED

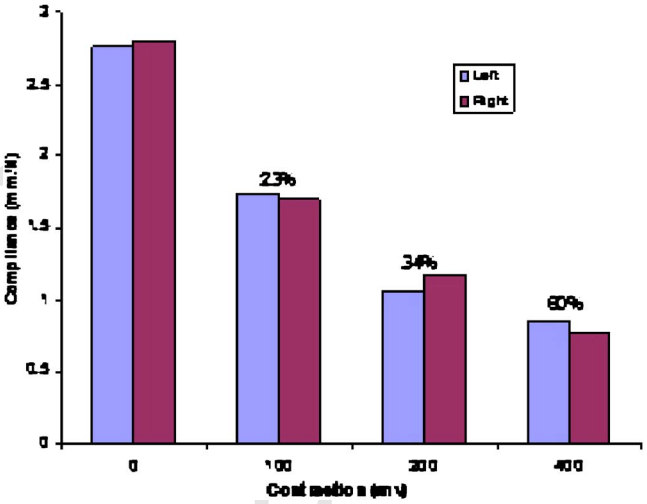

Fig. 11 Compliance with contraction, cervical region

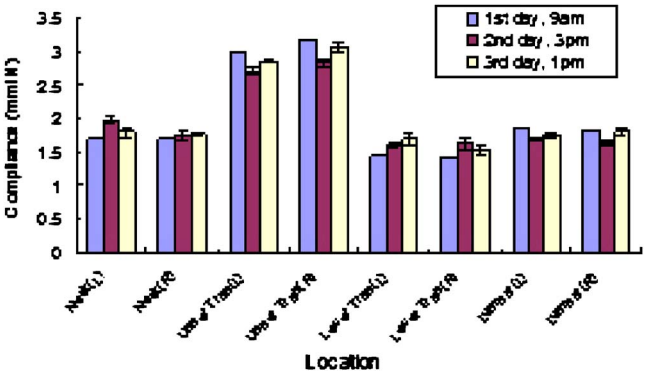

Fig. 12 Reproducibility results

measured in Fig. 10. If the measured compliance is significantly greater from the PHANTOM® compliance, the latter may be ignored. If the PHANTOM® compliance is a significant fraction of the equivalent measured compliance, then we may apply the correction of (2): the corrected compliance values are 1.35−0.44 =0.91 mm/N for the right and 1.27−0.37=0.90 mm/N or the left. The true results are less compliant than the measured results due to the PHANTOM® compliance. Taking into account the (different) compliances of the right and left PHANTOMS®, the (true) measured right and left side back compliances are nearly identical.

Figure 11 presents a typical compliance result in the cervical region (the lumbar and trapezius results are similar) with right and left measurement points and voluntary contractions to create progressively less compliant tissue. In Fig. 11, the percentage numbers indicate the percent contraction at each level. In this experiment, 400 mV corresponded to the maximum voluntary contraction. We see that increased voluntary contractions, leading to tenser tissue, can be measured by our system as reduced compliance.

These contracted muscle compliance measurement experimental results are from one subject only. They are included to demonstrate that our system may be used to detect tissue of altered compliance clinically, an area we think is promising for various biomedical applications.

3.3 Angled Compliance Measurements. We wish to measure compliance normal to the body surface at each point of interest. Therefore, we developed a method to measure the normal to the skin surface (manually using inclinometers in two planes) and then commanding the PHANTOM® to exert force along that normal rather than purely vertical. All results presented in this article make use of this method.

4 Compliance Measurement Issues

This section presents some important issues relating to our compliance measurement methods: reproducibility, seated versus prone measurements, the effect of thoracic (lung) volume, and the effect of different time intervals for the step changes in force.

4.1 Reproducibility. A crucial aspect of our measurement system is to ascertain if the measurements are reproducible, i.e., if we measure the compliance at the same point on the same person in the same manner, will we get the same answer (within reasonable limits)? This is complex since the subject may change from day to day and even by time of day so any changes in compliance measurement could be due to nonrepeatable measurements, changing tissue in the subject, or a combination.

For the same subject, this compliance test was repeated thrice at different times and on three consecutive days as shown in the legend of Fig. 12, for 8 back points (4 on the left and 4 on the right). For the first-day test, we just did one trial at each point, so there is no standard error bar for that data. Figure 12 shows that there are little compliance measurement differences on different days or different times of day. Our back compliance measurements are thus shown to be reproducible, at least for one subject. The differences in Fig. 12 are possibly equally due to subtle changes in the subject as due to measurement inaccuracies.

Since Fig. 12 is presented for only one subject and only three measurements at each location and time, we attempted no test of statistical significance.

4.2 Seated Versus Prone Back Compliance Measurements. We are also interested in how the compliance might change for measurements of the same point of seated (Fig. 13) versus prone (Fig. 2) subjects. We made an adjustable chair for the seated measurements (Fig. 13). 12 subjects were involved in this experiment, 6 female and 6 male. The order of the seated and prone measurements of each subject was chosen randomly. Three points T3, T7, and L3 (all offset 2 cm to the right of the spine) on the back of each subject were tested. The compliance at each point was tested four times and averaged. Since the spine curvature is generally different seated versus prone, the relative angles of T3, T7, and L3 are also different. We adjusted the chair and used pillows to make the subjects' spines as similar as possible seated and prone.

Figure 14 shows the seated versus prone compliance results. We averaged results over all subjects since there was no statistical difference between male and female subject compliances (with a 0.05 significance level). Figure 14 is a comparison of paraspinal tissue compliance measurements at the three-sites in both seated and prone positions with standard deviation bars shown. The asterisk indicates a significant difference ($P<0.05$). Table 5 summarizes the average compliance results for all 12 subjects for the six conditions.

The compliance of the upper back (T3) measured prone is less than that of the seated. The compliances of the middle back (T7) are about the same seated and prone because there is not much muscle change in this area going from seated to prone. The compliance of the lower back (L3) measured prone is greater than that of the seated.

4.3 Thoracic Volume Effect. Another question we need to address in making reliable tissue compliance measurements is what is the effect of thoracic volume on the measured compliance? That is, our subjects must hold their breath during all pseudostatic compliance measurements; otherwise, the respiration motion interferes with the displacement measurements. Is there an effect of how much breath is held (i.e., thoracic volume) on the resulting compliance measurement?

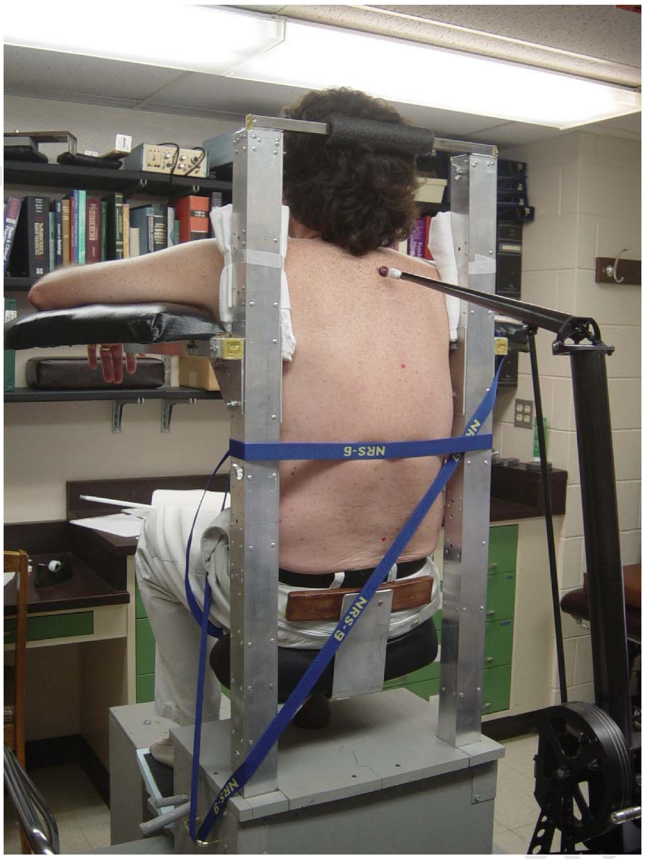

Fig. 13 Seated back measurements

There were ten subjects in this experiment, five female and five male. Each subject lay facedown on a table and controlled the level of his/her breath by watching a scope to which a chest respiration sensor was connected. Subjects were instructed to reach normal and maximum inhalation levels and two intermediate levels (2× and 3×) were identified. The static compliance measurements were made 2 cm to the right of vertebrae T3, T7, and L2.

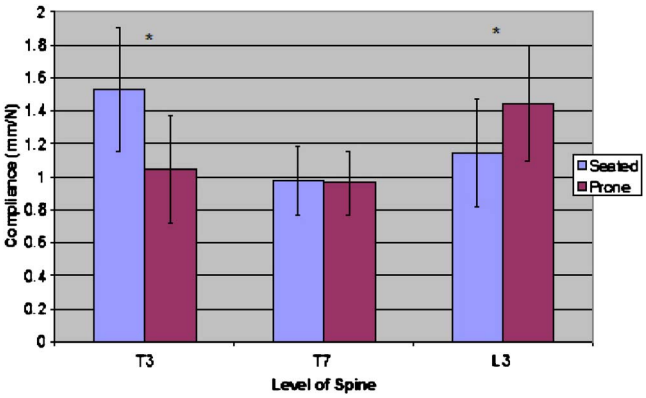

Fig. 14 Prone/seated compliance results

Table 5 Average prone/seated compliance results (mm/N; standard deviations in parentheses)

	T3	T7	L3
Seated	1.528 (0.372)	0.977 (0.210)	1.143 (0.323)
Prone	1.044 (0.328)	0.964 (0.195)	1.441 (0.351)

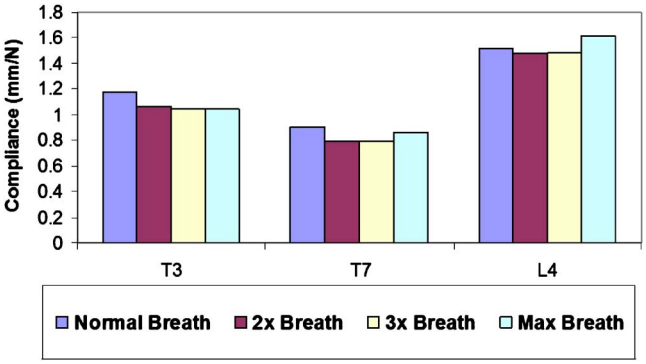

Fig. 15 Thoracic volume compliance results

Figure 15 shows average compliance results over all subjects to demonstrate the compliance trends with different breath levels, including standard error bars. Generally, increased thoracic volume (more breath held) means decreased measured compliance for most subjects, but the effect is very slight and not borne out for the maximum breath level. We did not find any significant gender differences.

Multivariate tests were used to analyze data from all trials at T3, T7, and L4 to determine if changes in respiratory volume made a significant difference in compliance. No significant differences were noted in the data at T3 ($P=0.444$), T7 ($P=0.518$), or L4 ($P=0.892$) between levels of respiration. The compliances of T3, T7, and L4 are all significantly different ($P<0.05$).

In the interest of subject comfort, and since there are no significant compliance differences over thoracic volume, we conclude that the normal comfortable breath level should be held for all compliance measurements. All other results presented in this article used the normal breath level.

4.4 Force Step Change Time Interval. As mentioned previously, our compliance measurement technique at a given point involves automatically changing the force command in steps and recording the displacement seven times while the subject holds her breath. This subsection looks at the effect of different time intervals of force step changes.

There were ten subjects in this experiment, five female and five male. We tested five points (all offset 2 cm to the right of the spine) on the back of each subject: T3, the midpoint between T3 and T7, T7, the midpoint between T7 and L3, and L3. At each point, the compliance test was repeated with different time intervals of 0.5 s, 1 s, 1.5 s, 2 s, 2.5 s, and 3 s. Figure 16 shows a typical result of the experiment at one test point (L3) for one

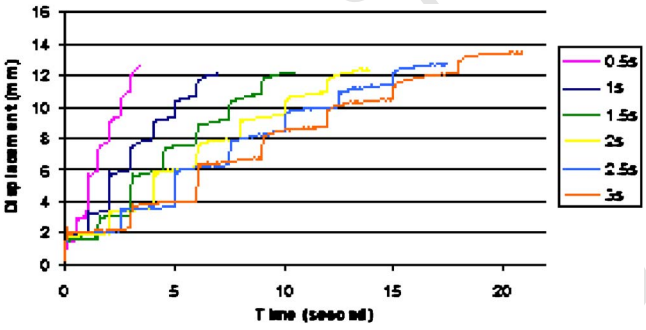

Fig. 16 Different force time intervals

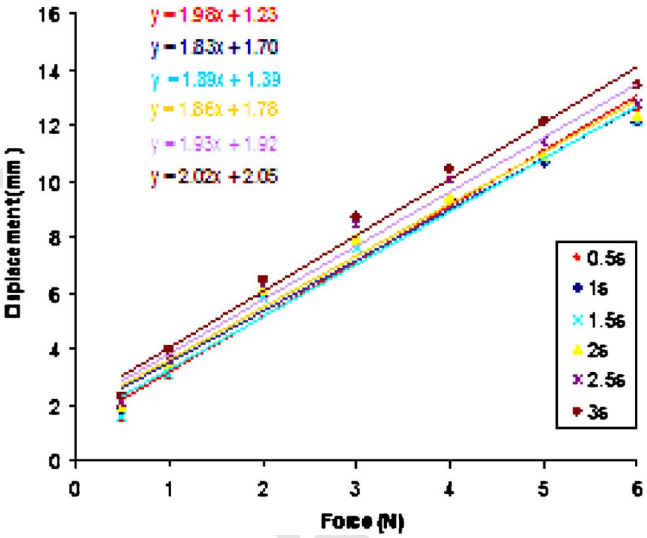

Fig. 17 Compliance lines for Fig. 16

subject with the six different force step time intervals.

The data of Fig. 16 are analyzed to generate the best-fit static compliance lines of Fig. 17, using displacement values near the end of each force step time interval. The slope of each best-fit line is the compliance determined for that particular time interval. Though some of the line intercepts vary, the slopes are very similar, indicating that there is not a strong effect of force time interval on compliance.

The compliance values of Fig. 17 are plotted in Fig. 18 versus the six force step time intervals for a single subject. We do not present any composite data in this experiment due to compliance variation amongst subjects. However, for each subject, the compliance varied little for the different force step time intervals. The single subject case shown in Fig. 18 is typical.

Since there is no strong effect of force time interval on measured compliance, we can choose any convenient time interval. The shorter the time interval, the more comfortable for the breath-holding subjects and the more data we can obtain in the same laboratory time. However, the longer the time interval, the more certain we are that tissue dynamics does not interfere and the recorded displacement value is the proper one (i.e., not increasing any longer). Therefore, we choose a time interval in the middle of the range considered, 1.5 s. This is the value used in all other results presented in this article. As we saw in Fig. 3, a force step time interval of 1.5 s can be borderline in terms of the displacement settling to a final value in time.

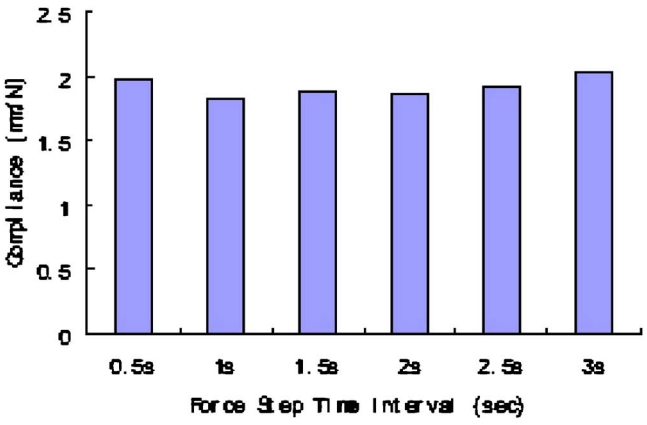

Fig. 18 Effect of force step time interval on compliance

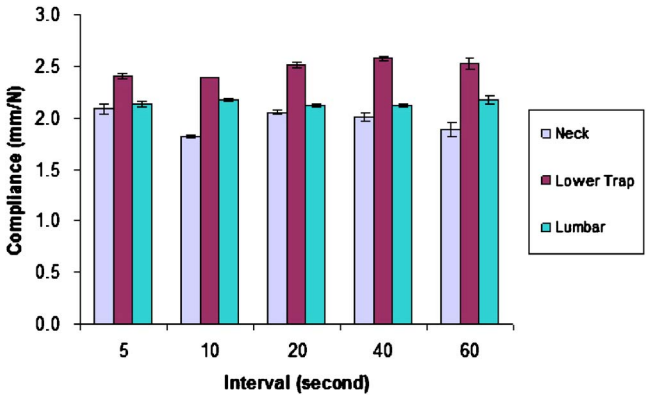

Fig. 19 Compliances versus waiting time intervals

4.5 Effect of Resting Time Between Compliance Tests. This test, with four subjects, is to determine the effect of different resting times between successive compliance measurements (as opposed to the time interval between force step changes used in one compliance measurement, considered in the previous subsection). Three test points were chosen on the subject back (neck, lower trapezius, and lumbar), each offset 2 cm to the right of the spine center. At each point, the compliance test was repeated four times (trials) with the same resting time interval between compliance measurements. We use the average of the last three trials as the result at each point because the first trial did not have any waiting interval. Then, we repeated this procedure at the second and third back points. After testing the three points in this manner, the waiting time interval was increased. We used waiting time intervals of 5 s, 10 s, 20 s, 40 s, and 60 s. Figure 19 shows a typical result for one subject, with standard error bars over the trials. Each group of columns displays the compliances of three back points with the same waiting time interval.

From the data of Fig. 19, typical of all subjects, we do not see significant differences in measured compliance over the waiting time interval. Thus, we may use whatever waiting time interval is convenient in the laboratory for each measurement. All other results presented in this article were obtained without controlling the waiting time interval.

5 Summary

This article has presented our methods for in vivo measurement of human tissue compliance using our softcometer. We use PHANTOM® 3.0 haptic interfaces to exert a series of known force levels at each point of interest while the subject is immobile and holding her breath while relaxed. The PHANTOM® measures the associated displacements, from which compliance curves are automatically generated by the computer. We use this information to improve the haptic realism of our virtual haptic back model (used for training medical students in palpatory diagnosis at Ohio University), but this type of information is useful in various applications.

We presented our pseudostatic compliance measurement techniques, with sample results including with voluntary muscle contractions to simulate compliance measurements of contracted muscles. We demonstrated that our method can measure different voluntary muscle contraction levels, indicating that it will also be effective for clinicians measuring muscle tone clinically where muscle compliance is a concern. We focused only on pseudostatic compliance measurement; development of viscoelastic dynamic models for human tissue is the subject of future work.

We also discussed several important issues related to our in vivo measurement techniques. Our method was shown to be reproducible over different days and times of the day. Compliance characteristics vary for different back points in seated versus prone subjects. The thoracic volume effect was shown to decrease

compliance as more breath was held; therefore, we use only the normal breath level. The effect of time intervals between applied force steps was shown and we compromised on an intermediate value of 1.5 s. There was no effect of waiting time interval on successive compliance measurements.

Our in vivo human tissue compliance measuring method may be extended to other parts of the human anatomy in addition to the back. This method can be used by biomedical researchers, industrial ergonomic designers, and clinical medical personnel.

Acknowledgment

We gratefully acknowledge financial support for this research from the Osteopathic Heritage Foundation. Thanks to David Noyes for intellectual contributions and for construction of the adjustable measurement chair. Ohio University medical students Bobbi Rockey and Maria Streng are also acknowledged for their data collection in the seated versus prone and thoracic volume compliance measurement experiments, respectively.

References

[1] Williams, R. L., II, Srivastava, M., Conatser, R. R., Jr., and Howell, J. N., 2004, "Implementation and Evaluation of a Haptic Playback System," Haptics-e Journal, IEEE Robotics & Automation Society, 3(3), pp. 1–6.

[2] Noyes, D. H., and Solt, C. W., 1977, "Elastic Response of the Temporomandibular Joint to Very Small Forces," J. Periodontol., **48**, pp. 98–100.

[3] Ottensmeyer, M. P., 2002, "In Vivo Measurement of Solid Organ Viscoelastic Properties," Stud. Health Technol. Inform., **85**, pp. 328–333.

[4] Wang, J., Brienza, D. M., Yuan, Y., Karg, P., and Xue, Q., 2000, "A Compound Sensor for Biomechanical Analysis of Buttock Soft Tissue In Vivo," J. Rehabil. Res. Dev., **37**(4), pp. ■–■.

[5] Edsberg, L. E., Mates, R. E., Baier, R. E., and Lauren, M., 1999, "Mechanical Characteristics of Human Skin Subjected to Static Versus Cyclic Normal Pressures," J. Rehabil. Res. Dev., **36**(2), pp. ■–■.

[6] Bruyns, C., and Ottensmeyer, M. P., 2002, "Measurements of Soft-Tissue Mechanical Properties to Support Development of a Physically Based Virtual Animal Model," *Proceedings of the Fifth International Medical Image Computing and Computer-Assisted Intervention Conference (MICCAI)*.

[7] Carter, F. J., Frank, T. G., Davies, P. J., McLean, D., and Cuschieri, A., 2001, "Measurements and Modeling of the Compliance of Human and Porcine Organs," Med. Image Anal, **5**, pp. 231–236.

[8] Djerad, S. E., du Burck, F., Naili, S., and Oddou, C., 1992, "Analyse du Comportement Rhéologique Instationnaire d'un Échantillon de Muscle Cardiaque," C. R. Acad. Sci., Ser. II: Mec., Phys., Chim., Sci. Terre Univers, **315**, pp. 1615–1621.

[9] Randolph, R. G., 1977, "Durometer for Indentible Tissue and the Like," U.S. Patent No. 4,132,224.

[10] Kovacevic, N., 1994, "Skin Compliance Measurement Device," U.S. Patent No. 5,373,730.

[11] Neurogenic Technologies, Inc., "The Myotonometer®," www.neurogenic.com

[12] Arokoski, J. P., Surakka, J., Ojala, T., Kolari, P., and Jurvelin, J. S., 2005, "Feasibility of the Use of a Novel Soft Tissue Stiffness Meter," Physiol. Meas, **26**, pp. 215–228.

AQ: #4 AQ: #5 AQ: #6

PROOF COPY [MED-06-1067] 005703MED

AUTHOR QUERIES — 005703MED

#1 Au: Please check changes made in the byline.

#2 Au: ALL REFERENCES MUST BE CITED IN TEXT. PLEASE CHECK OUR INSERTION OF REF. 12.

#3 Au: PLEASE DEFINE “EMG.” IF POSSIBLE.

#4 Au: PLEASE CHECK CHANGES MADE IN REFS. 1, 3, AND 6. Au: PLEASE SUPPLY THE FULL JOURNAL TITLE, THE CODEN, AND/OR ISSN IN REF. 1.

#5 Au: PLEASE CHECK JOURNAL TITLE IN REFS. 2 & 8

#6 Au: PLEASE SUPPLY PAGE RANGE IN REFS. 4 AND 5.